# Vacancy defects in CdTe thin films

D. J. Keeble,[1,*] J. D. Major,[2] L. Ravelli,[3] W. Egger,[3] and K. Durose[2]

[1]*Carnegie Laboratory of Physics, SUPA, School of Engineering, Physics, and Mathematics, University of Dundee, Dundee, DD1 4HN, United Kingdom*

[2]*Stephenson Institute for Renewable Energy, University of Liverpool, Liverpool, L69 7ZF, United Kingdom*

[3]*Universität Bundeswehr München, D-85577 Neubiberg, Germany*

(Received 17 August 2011; revised manuscript received 7 November 2011; published 23 November 2011)

Vacancy defects have been investigated in a series of CdTe thin films grown by close-space sublimation. Variable-energy positron annihilation lifetime spectroscopy measurements, performed with a high-intensity positron beam, were used to profile polycrystalline films with varying grain size. These were obtained by changing the nitrogen pressure used during deposition. Two vacancy defects were detected, with positron lifetimes of 321(7) ps and 450(30) ps, respectively. Density functional theory calculations support the assignment of the first to the Cd vacancy and provide evidence that the second is the divacancy defect.

DOI: 10.1103/PhysRevB.84.174122 PACS number(s): 78.70.Bj, 61.72.jd, 88.40.jm

## I. INTRODUCTION

Cadmium telluride combines a number of desirable properties, making it a focus of interest for several important applications, ranging from solar cells to medical imaging devices. The 1.5-eV bandgap provides an excellent match to the solar spectrum, and the addition of Zn ($Cd_{1-x}Zn_xTe$) allows this value to be controllably increased. The relatively high average atomic number combined with the potential for high resistivity makes it ideal for gamma- and x-ray detector devices. It should also be noted that CdTe is one of the few II-VI semiconductors that can be doped both $n$ and $p$ type. However, actual material performance can be compromised by the presence of native and impurity ion point defects, reducing resistivity and degrading photovoltaic device performance. Controversy has developed during the last decade regarding point defect identification in CdTe. Electron paramagnetic resonance (EPR) observed two paramagnetic centers thought to be due to native defects, an isotropic center originally attributed to the Te vacancy[1,2] but more recently assigned to the Te antisite,[3] and a trigonal center with the unpaired spin density localized on a single Te originally identified as the Cd vacancy, $V_{Cd}$, exhibiting a strong Jahn–Teller (JT) distortion.[2] Subsequently a number of first-principles calculations have been reported,[4–6] none of which supports the existence of a strongly distorted paramagnetic charge state for $V_{Cd}$. However, other point defect sensitive local probe spectroscopy methods, specifically perturbed angular $\gamma$-$\gamma$ correlation (PAC) spectroscopy and positron annihilation lifetime spectroscopy (PALS) have identified Cd vacancy defects.[6–10]

Here, we report depth profiled positron lifetime measurements of the near-surface regions of CdTe thin films, performed using a high-intensity variable-energy positron beam. The observed lifetime components were found to be consistent with previous PALS measurements on bulk CdTe samples. The $V_{Cd}$ lifetime was resolved and a second defect with a longer lifetime detected. Density functional theory (DFT) calculations of positron lifetimes were performed, and these supported the assignment of the $V_{Cd}$ lifetime and provided evidence that the longer lifetime component can be attributed to the divacancy defect.

An implanted positron will thermalize within a few picoseconds then annihilate in the material from a state $i$ with a lifetime $\tau_i$ and a probability $I_i$. This can be a delocalized state in the bulk lattice or a localized state at a vacancy defect, or if the open-volume defect has sufficient size (e.g. in nanovoids), the electron-positron-bound state known as positronium can be formed. The presence of vacancy-type defects is indicated if the average lifetime, $\bar{\tau} = \sum_i I_i \tau_i$, is greater than the bulk (perfect lattice) lifetime, $\tau_B$, characteristic of the material. The rate of positron trapping to a vacancy, $\kappa_d$, is proportional to the concentration of these defects, $[d]$, where the constant of proportionality is the defect-specific trapping coefficient, $\mu_d$; $\kappa_d = \mu_d[d]$. While vacancy defects, due to the lack of a positive ion core, form an attractive potential, the local charge must also be considered; if positive, a Coulomb barrier inhibits trapping; however, for neutral or negative defects, trapping coefficients are large, typically in the range 1–10 $\times$ $10^{15}$ $s^{-1}$, giving the method a sensitivity of typically better than $10^{16}$ $cm^{-3}$.[11]

The one-defect standard trapping model (STM) predicts two experimental positron lifetimes; $\tau_2 = \tau_d$ is the lifetime characteristic of the defect, and the first lifetime, $\tau_1$, is reduced below the perfect lattice lifetime by an amount that depends on the rate of trapping to the defect so that $\tau_1 \leqslant \tau_B$ and is termed the reduced bulk lifetime. The defect positron trapping rate, $\kappa_d$, can be calculated from the measured lifetime values and intensities.[11] The model is readily extended to two or more defects and results in the appropriate number of additional fixed defect lifetime components in the spectrum. As the concentration of vacancies increases, both the lifetime and intensity of the reduced bulk component decrease. In the limit, termed saturation trapping, the reduced bulk component is not resolved, and essentially all positrons annihilate from the defects. An upper limit of defect concentration, $[d]$, beyond which positron lifetime measurements alone lose sensitivity to absolute concentration, is defined; assuming a specific trapping coefficient $\sim$0.7 $\times$ $10^{15}$ $s^{-1}$ and $\tau_B$ = 290 ps, a value of the order of 4 $\times$ $10^{17}$ $cm^3$ ($\kappa_d\tau_B = \mu_d[d]\tau_B \approx 10$) is predicted.

The positron lifetimes for perfect material and for specific vacancy defects can be calculated using density functional theory (DFT) methods.[12] The results of previous calculations of lifetime values for CdTe, performed using the atomic

 

TABLE I. Positron lifetime values (ps) calculated by the DFT using MIKA-Doppler for monovacancy, divacancy, and four-vacancy cluster defects in CdTe.

| | BN | AP | Ref. 13 |
|---|---|---|---|
| Bulk | 276 | 309 | 276 |
| $V_{Cd}$ | 291 | 322 | 288 |
| $V_{Te}$ | 307 | 343 | 301 |
| $V_{Cd}V_{Te}$ | 355 | 417 | 355 |
| $2(V_{Cd}V_{Te})$ | 398 | 503 | |

superposition DFT method within the local density approximation (LDA), are included in Table I.[13] It is well known these calculations underestimate the experimental values, and hence scaling approaches have been explored.[9,13] Positron lifetime studies on bulk crystal CdTe have provided evidence that the bulk lifetime is in the range of 280(1) ps to 287 ps.[8,9] Measurements of In-doped CdTe have identified a defect lifetime at 320(5) ps attributed to either $V_{Cd}^{2-}$ or $(V_{Cd}In_{Cd})^{-}$ complexes.[7,14] This assignment was supported by a subsequent study which reported trapping to $V_{Cd}$-related defects with a lifetime of 323(3) ps.[8] In contrast, measurements of Cl-doped CdTe identified a second positron lifetime in the range of 350–395 ps,[15] and in separate studies, values of 370(5) ps and 381 ps were reported.[8,16] However, subsequent higher-statistics PALS measurements on CdTe:Cl crystals provided evidence that the ∼350–395 ps component was in fact an unresolved weighted average of two defect contributions, one at 330(10) ps and one at 450(15) ps.[9,11] The former attributed to $(V_{Cd}Cl_{Cd})^{-}$ complexes, and the 450-ps component was assigned, on the basis of the $\tau_B/\tau_d$ ratio, to a divacany or larger open-volume defect.

Positron annihilation studies of thin film CdTe have been restricted to variable-energy Doppler broadening spectroscopy (VE-DBS) detected measurements,[8,16–18] where the annihilation radiation gamma-ray energy spectrum is characterized using the lineshape parameters $S$ and $W$. In a careful study of both bulk samples and evaporated CdTe films, it was possible to infer from the large $S$ values in the films combined with the trends observed in $S$-$W$ plots that divacancy defects were likely present in the films.[18] However, DBS spectra cannot normally identify individual contributions when more than one defect type is present.

## II. EXPERIMENT

The CdTe films studied were grown by close-space sublimation (CSS); the nitrogen pressure during deposition was varied to control grain size.[19] The substrates were $SnO_2$:F-coated soda-lime glass (Pilkington TEC15) with a room temperature sputtered ZnO high-resistance transparent conducting oxide layer and a 120-nm CdS buffer layer deposited by RF sputtering at 200 °C in argon. The CSS depositions were carried out using source and substrate temperatures of 615 and 520 °C, respectively. Three films were grown using the nitrogen chamber pressures, 5, 20, and 100 Torr; the growth times were adjusted to give ∼10 $\mu$m films. The subsequent $CdCl_2$ annealing step typically used in solar cell fabrication was omitted.[19] The samples were then polished to reduce surface roughness.

Positron annihilation measurements were performed at the high-intensity neutron-induced positron source (NEPOMUC) at the Munich research reactor FRMII with a primary moderated beam intensity of $5 \times 10^8$ $e^+$ $s^{-1}$ at an energy of 1 keV.[20] Variable-energy (VE) positron annihilation lifetime spectroscopy (PALS) measurements were made with the pulsed-beam instrument comprising a prebuncher, chopper, and main buncher operating at 50 MHz providing the time structure and start timing signal; the annihilation radiation from the implanted positrons was detected using a $BaF_2$ scintillation detector.[21] The lifetime spectra contained greater than $4.8 \times 10^6$ counts; the instrument timing resolution function was normally described by three dominant energy-dependent terms; these showed a mean width, averaged over all energies, of 273 ps. Spectra were measured using positron implantation energies of 1, 4, 8, and 18 keV.

Positron lifetime calculations were performed using density functional theory (DFT) method implemented in the MIKA/Doppler package,[22] where the electron density of the solid is approximated by the nonself-consistent superposition of free atom electron densities in the absence of the positron (the so-called conventional scheme).[12] Calculations of the positron lifetimes were performed using an electron-positron enhancement factor obtained from the data of Arponen and Pajanne,[23] both the original by parameterization by Boroński and Nieminen (BN),[24] described within the local density approximation (LDA), and with a more recent expression obtained by Barbiellini *et al.*[25,26] (referred to as AP), described within the generalized gradient approximation (GGA). The LDA calculations using BN enhancement assumed a value of 7.1 for the CdTe high-frequency dielectric constant. Positron lifetime calculations were performed for unrelaxed monovacancy defects, the divacancy, and a four-vacancy cluster using 1,000-atom $5 \times 5 \times 5$ supercells.

## III. RESULTS AND DISCUSSION

The average grain size of the CSS-deposited CdTe films were measured by scanning electron microscopy, see Fig. 1, and found to be 1.3(6), 3.7(1.5), and 5.3(2.6) $\mu$m for the 5, 20, and 100 Torr films, respectively.

The variation of the mean positron lifetime, $\bar{\tau}$, with positron implantation energy for the three CdTe films is shown in Fig. 2. These values were all significantly larger than the CdTe bulk positron lifetime of ∼285 ps,[8,9] indicating the presence of vacancy-related defects. The near-surface 1-keV implantation energy spectra from all three films gave similar mean positron lifetimes (∼340 ps). However, at the higher implantation energies, the mean lifetimes for the 5-Torr film were larger than the 20- and 100-Torr grown film values; the 20- and 100-Torr film $\bar{\tau}$ values were comparable. The mean values were all equal to or greater than the $V_{Cd}$ lifetime (∼320 ps),[7–9,14] providing evidence for the presence of larger open-volume defects.

The high statistics obtained from the intense reactor-based positron beam allowed the PALS spectra to be deconvolved using multiexponential fitting. The results for the 1-keV implantation energy spectra from the three films are given in Table II. The experimental PALS spectrum for the 100-Torr

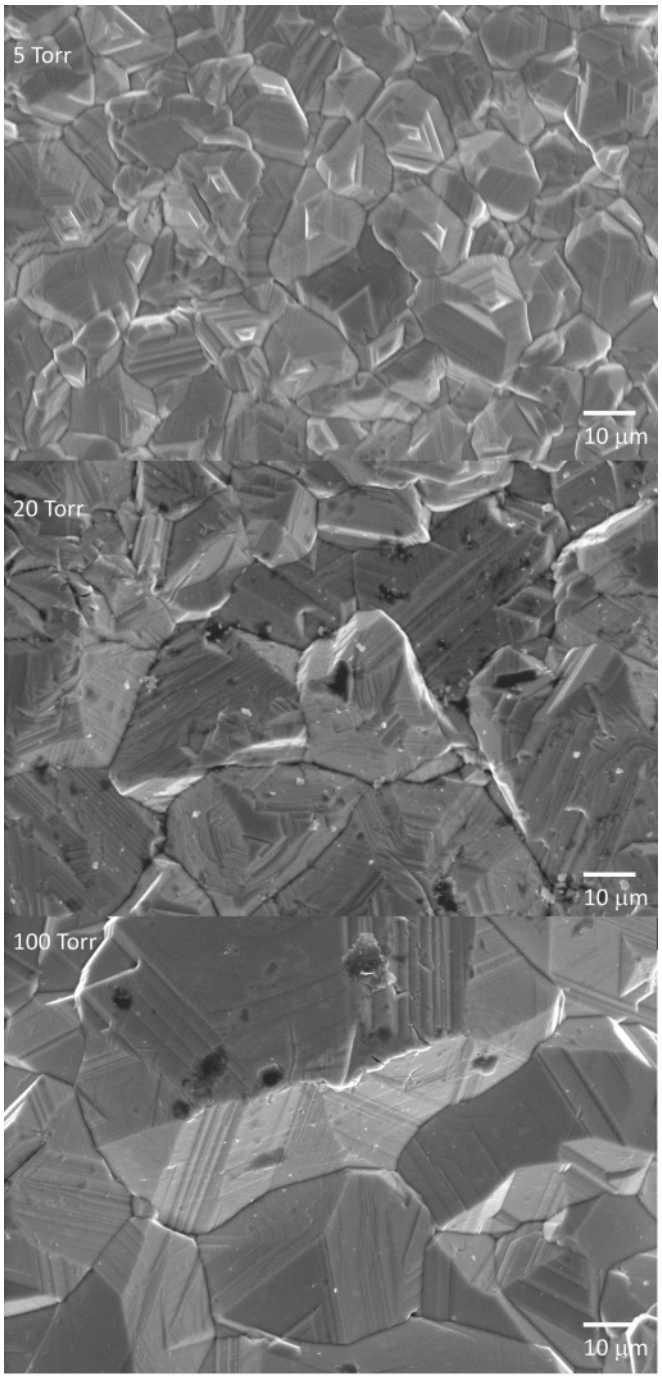


FIG. 1. Scanning electron microscopy images of close-space sublimation-deposited CdTe thin films grown with 5-, 20-, and 100-Torr nitrogen growth chamber pressures.

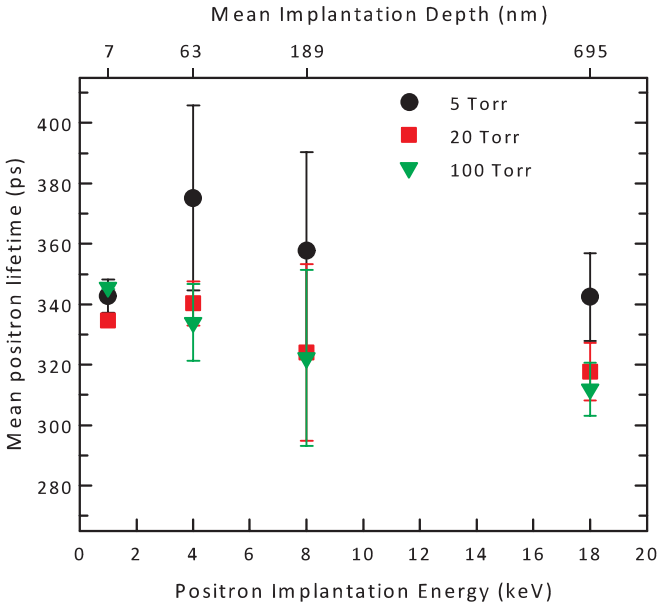


FIG. 2. (Color online) Mean positron lifetimes against positron implantation energy, measured by variable-energy positron beam positron annihilation lifetime spectroscopy for CdTe thin films grown with 5-, 20-, and 100-Torr nitrogen growth chamber pressures.

grown film is shown in Fig. 3, with associated fits from Table II. The three-term fits of the 1-keV spectra gave a first lifetime component at $<100$ ps, a dominant second component in the range of $\sim$350–370 ps, and a third $\sim$1–2-ns lifetime with an intensity of $\sim$1%. The presence of a long lifetime positronium component was clearly observed in the 1-keV spectra,[27] in contrast to the higher implantation energy spectra. The mean implantation depth for 1 keV is only $\sim$7 nm, hence a fraction of positrons back-diffuse to the surface and result in positronium formation. Fitting the spectra to four lifetimes resulted in two significant defect contributions for the 20- and 100-Torr films, one at 321(9) ps and a second at 441(26) ps, and showed significantly improved fit chi-squared values. For the 5-Torr grown film, it was necessary to fix one of the four component lifetimes at 321 ps to obtain a comparable fit. The four-term fit results are in agreement with the earlier high-statistics PALS study of Cl-doped CdTe bulk crystals in which an initial observed defect component in the 350–395-ps range was shown to be due to two defect lifetimes, one at 330(10) ps and one at 450(15) ps.[9]

The results reported here add to the substantial number of observations of a vacancy defect positron lifetime in the range of 320–330 ps in CdTe.[7–9,14,28] This is attributed to the $V_{Cd}$ defect, either isolated and in the two-charge state or with a near neighbor substitutional donor. The results of the DFT calculations of positron lifetimes in CdTe are shown in Table I. The lifetime values obtained here using LDA with BN enhancement are in excellent agreement with similar earlier calculations.[13] The calculated increase in the lifetime for $V_{Cd}$ compared to the bulk of 1.05 is comparable to the experimental value of $\sim$1.12. However, the absolute values for the bulk and $V_{Cd}$ of 276 and 291 ps, respectively, are smaller than the experimental lifetimes ($\sim$285 and $\sim$320 ps, respectively). The GGA calculations using AP enhancement give a bulk lifetime of 309 ps, which is higher than the experimental value, but the resulting $V_{Cd}$ lifetime value of 322 ps is in close agreement with experiment.

The calculated $V_{Cd}V_{Te}$ divacancy values were 355 and 417 ps using the LDA-BN and GGA-AP approaches, respectively (Table I); the four-vacancy cluster $2(V_{Cd}V_{Te})$ was also studied and gave values of 398 and 503 ps, respectively. There is approximate agreement between the 417-ps GGA-AP calculated divacancy lifetime and the second defect component at 441(26) ps, shown in Table II. The closer correspondence

TABLE II. The positron lifetime component values obtained from the 1-keV implantation energy PALS spectra for the three CdTe thin films grown with different nitrogen pressures ($P$). The results of three- and four-term fits are given, $F$ denotes a value fixed during the fitting.

| $P$(Torr) | $\tau_1$ | $\tau_2$ | $\tau_3$ | $\tau_4$ | $\chi^2$ |
|---|---|---|---|---|---|
| 100 | 48(2) ps, 7.4(2)% | 353(1) ps, 91.6(2)% | 1.99(3) ns | | 1.296 |
| 100 | 16(2) ps, 7.5(3)% | 319(8) ps, 67(9)% | 439(25) ps, 24(9)% | 2.74(7) ns | 1.106 |
| 20 | 53(3) ps, 7.3(1)% | 358(1) ps, 91.5(1)% | 2.10(3) ns | | 1.310 |
| 20 | 17(2) ps, 7.4(2)% | 323(9) ps, 67(10)% | 443(26) ps, 25(10)% | 2.68(6) ns | 1.061 |
| 5 | 51(3) ps, 6.0(2)% | 374(1) ps, 92.6(1)% | 1.38(9) ns | | 1.282 |
| 5 | 30(3) ps, 5.6(2)% | 355(3) ps, 83(3)% | 555(28) ps, 11(3)% | 3.8(2) ns | 1.072 |
| 5 | 18(3) ps, 5.8(4)% | 321($F$) ps, 51(1)% | 441(3) ps, 43(1)% | 2.8(1) ns | 1.096 |

between the experimental defect lifetimes and the GGA-AP-calculated values provides some support for the divacancy assignment. Further, the four-vacancy cluster defect results in a GGA-AP-calculated lifetime that is significantly larger than the ∼450 ps experimental value. It should be noted that first-principles determinations of the local atomic relaxations for vacancy-related defects in CdTe would allow calculations of the positron lifetime values of the relaxed defects. This has been found to result in improved agreement with experiment for the wide bandgap oxide materials.[29]

The detailed PALS spectrum fits for the three CdTe films for the implantation energies 4–18 keV are given in Table III. The three-term fits resulted in a dominant second lifetime component in the range 290 to 368 ps with an intensity varying from ∼55 to 85%, a first lifetime in the ∼70- to 120-ps range with an intensity between ∼5 to 10%, and a third lifetime in the range 450 to 800 ps and an intensity between 37 to 2%. Several

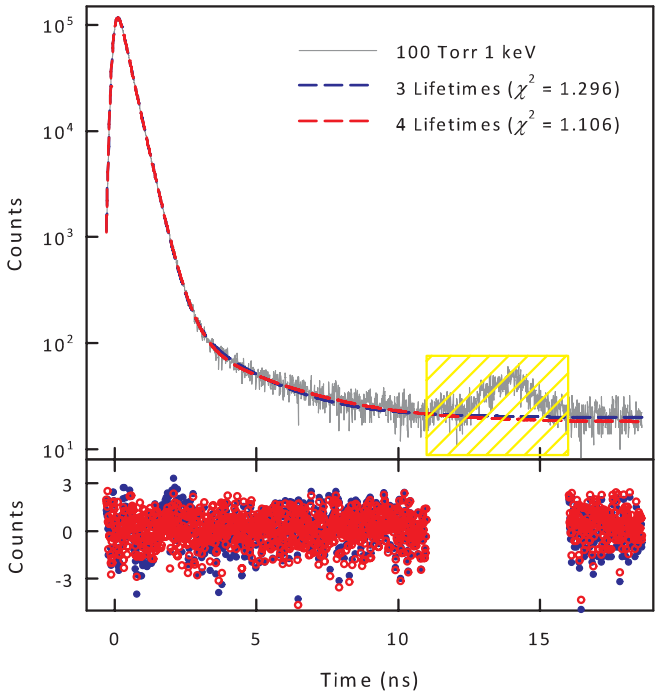


FIG. 3. (Color online) VE-PALS spectrum for the 100-Torr nitrogen grown CdTe thin film using 1-keV positron implantation energy. The highlighted region (yellow shading/lined rectangle) is due to a positron reflection and was excluded from fits. Both three (blue/medium gray) and four term (red/dark gray) fits are shown, and the associated fit residuals are plotted in the lower panel.

of these fits give a second lifetime component value close to 320 ps, the $V_{Cd}$ value. Increasing the number of fitted positron states to four but constraining one lifetime value to 321 ps gave improved fit chi-squared values. In the majority of cases, a third lifetime component consistent with the 441(26) ps value observed in Table II was also obtained. The fourth nanosecond lifetime component had negligible intensity (<0.5%).

The 20- and 100-Torr 18-keV PALS spectra did not yield stable four-term fits, see Table III. These samples exhibited the lowest mean lifetimes at this implantation energy, see Fig. 2, in contrast to the 5-Torr spectrum. It should also be noted that the relatively high average atomic number resulted in an increase in reflection artifacts with implantation energy; while this tended to shorten the time window at least 5 ns was always available, which was sufficient to allow accurate fitting.

The STM calculated bulk lifetime, $\tau_B^{\mathrm{STM}} = (\sum I_j/\tau_j)^{-1}$, calculated from the 4–18-keV four-term fits was 290(4) ps, and the three-term fit value was 286(9) ps. These are consistent with the previously reported experimental CdTe bulk positron lifetime range of 280(1) to 287 ps.[8,9] The 1-keV fits were excluded from the calculations due to the observed surface contribution; further, the instrument resolution function was broadest for this energy, which introduces larger uncertainties in the short lifetime component lifetime and intensity values. In addition, the 5-Torr film 4 keV value was found to be significantly larger (∼325 ps) and was excluded. In principle, defect concentrations can be obtained from the positron trapping rates calculated using the STM. Krause-Rehberg *et al.*[9] report defect-specific trapping coefficients for the Cd vacancy and for the possible divacancy defect of $9 \times 10^{14}$ and $1.8 \times 10^{15}$ s$^{-1}$, respectively. Using these values and the four-term STM fits, the estimated Cd vacancy and divacancy concentrations are ∼5–9 $\times 10^{16}$ and ∼1–4 $\times 10^{16}$ cm$^{-3}$, respectively.

Insight on the variation of defect populations between the films and as a function of depth can obtained from the four lifetime component fit results shown in Tables II and III, along with the variation in mean lifetimes shown in Fig. 2. Figure 4 shows the two dominant defect lifetime components from the appropriate four lifetime fits. These results show that the behavior of the 100- and 20-Torr samples were comparable, despite the reduction in grain size from 5.3(2.6) to 3.7(1.5) $\mu$m. The intensity of the 321-ps component was approximately 70%, while the intensity of the ∼450-ps component was approximately 20% (see Fig. 4). On reducing the grain size further to 1.3(6) $\mu$m for the 5-Torr sample, an increase in the intensity of the ∼450-ps component to ∼40% was observed, with a concomitant reduction in the $V_{Cd}$ component intensity to ∼55%.

TABLE III. Thin film CdTe positron lifetime component values for PALS spectra at positron implantation energies of 4, 8, and 18 keV for films grown with 5-, 20-, and 100-Torr growth chamber pressures. The results of three- and four-term fits are given, $F$ denotes a value fixed during the fitting.

| $P$(Torr) | $E$(keV) | $\tau_1$ | $\tau_2$ | $\tau_3$ | $\tau_4$ | $\chi^2$ |
|---|---|---|---|---|---|---|
| 100 | 4 | 108(6) ps, 8.7(6)% | 337(3) ps, 85(1)% | 618(22) ps | | 1.044 |
| | | 97(10) ps, 7(1)% | 315(30) ps, 69(32)% | 444(32) ps, 23(32)% | 1.0(3) ns | 1.033 |
| | | 111(9) ps, 7.8(6)% | 321($F$) ps, 73(4)% | 462(21) ps, 19(3)% | 1.2(2) ns | 1.021 |
| 100 | 8 | 113(7) ps, 7.5(3)% | 321(4) ps, 82(1)% | 544(21) ps | | 1.104 |
| | | 154(11) ps, 13(2)% | 321($F$) ps, 68(8)% | 443(32) ps, 18(6)% | 1.5(3) ns | 1.018 |
| 100 | 18 | 95(8) ps, 6.5(6)% | 303(3) ps, 85(1)% | 569(15) ps | | 1.209 |
| 20 | 4 | 127(6) ps, 11(1)% | 353(2) ps, 87(1)% | 793(31) ps | | 1.018 |
| | | 98(7) ps, 6.9(5)% | 321($F$) ps, 69(4)% | 450(20) ps, 24(3)% | 1.1(2) ns | 1.004 |
| 20 | 8 | 66(6) ps, 5.4(4)% | 290(5) ps, 67(3)% | 449(9) ps | | 1.043 |
| | | 111(5) ps, 8.9(4)% | 321($F$) ps, 79(1)% | 508(12) ps, 12(1)% | 12(9) ns | 1.068 |
| 20 | 18 | 131(8) ps, 10(1)% | 319(3) ps, 85(1)% | 656(22) ps | | 1.104 |
| 5 | 4 | 117(8) ps, 6.9(6)% | 368(5) ps, 82(2)% | 601(21) ps | | 1.117 |
| | | 85(9) ps, 4.4(3)% | 321($F$) ps, 53(1)% | 470(5) ps, 43(2)% | 1.8(2) ns | 1.047 |
| 5 | 8 | 68(5) ps, 6.2(3)% | 316(7) ps, 57(4)% | 469(9) ps | | 1.054 |
| | | 77(5) ps, 6.7(2)% | 321($F$) ps, 56(2)% | 464(5) ps, 37(1)% | 4(1) ns | 1.035 |
| 5 | 18 | 108(5) ps, 10(1)% | 347(4) ps, 82(1)% | 594(25) ps | | 1.024 |
| | | 100(6) ps, 9(1)% | 321($F$) ps, 59(7)% | 435(3) ps, 32(5)% | 0.9(3) ns | 1.023 |

The positron diffusion length, $L_+$, at room temperature for semiconductors is typically in the range of ~150–250 nm; the introduction of positron trapping defects reduces this value.[11] The one-defect STM predicts that $L_+$ varies with $\sqrt{\tau_1/\tau_B}$. The possibility of trapping to open-volume defects at the grain boundaries should be considered. The fraction of positrons reaching the grain boundaries, assuming homogenous positron implantation and thermalization, can be estimated using the analytical approach given by Brandt *et al.*[30] and Gainotti *et al.*,[31] noting that $L_+ = \sqrt{2dD_+\tau_{\text{eff}}}$ where $d$ is the dimensionality, $D_+$ the positron diffusion coefficient, and $\tau_{\text{eff}}$ the effective positron lifetime. Comparison of the predications of the model with the results of Monte Carlo simulations of positron diffusion showed the analytical expression slightly overestimates the grain boundary fraction.[32,33] Assuming $L_+ = 150$ nm, the fraction of positrons reaching the grain boundaries is calculated to be ~2, 5, and 14% for the 100-, 20-, and 5-Torr grown films, respectively. The intensity of trapping to the ~450-ps divacancy component is comparable for the 100- and 20-Torr films; this intensity approximately doubles to ~40% for the 5-Torr film. This increase in the intensity could be due to a homogenous increase in divacancy concentration due to changes in the growth kinetics on changing the nitrogen pressure or could indicate an enhanced concentration of these defects associated with the grain boundaries.

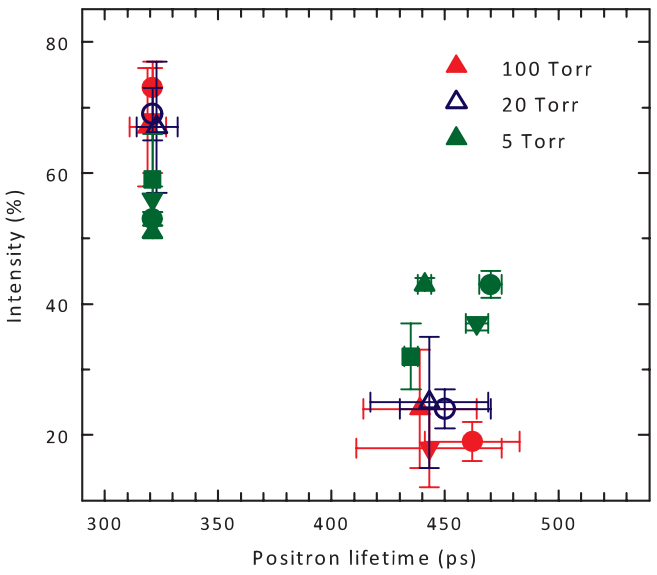


FIG. 4. (Color online) The dominant defect lifetime components selected from the VE-PALS spectrum four-lifetime component fits for the three CdTe thin films given in Table II and Table III. The implantation energies 1 keV (up triangle), 4 keV (circle), 8 keV (down triangle), and 18 keV (square, 5 Torr only) are shown.

## IV. CONCLUSIONS

In conclusion, variable-energy positron lifetime measurements identify the presence of Cd vacancy defects and larger open-volume defects in the near-surface region of a series of close-space sublimation-grown CdTe thin films grown with varying nitrogen pressures and hence grain sizes. Two defect positron lifetimes were observed in each film, the $V_{\text{Cd}}$ lifetime of 321(3) ps and longer lifetime at 450(30) ps. Density functional theory calculations of positron lifetimes in CdTe were performed; they provided good agreement for $V_{\text{Cd}}$ and supported the assignment of the second lifetime to divacancy defects. The concentrations of both defects was observed to be similar for the 100-Torr, 5.3(2.6)-$\mu$m grain size and 20 Torr, 3.7(1.5) $\mu$m, but increased positron trapping to divacancies was observed in the 5-Torr, 1.3(6), $\mu$m, film.

**ACKNOWLEDGMENTS**

D.J.K. acknowledges the support of the European Commission Programme RII3-CT-2003-505925. We thank C. Hugenschmidt for providing the NEPOMUC beamline. D.J.K. thanks I. Makkonen, Helsinki University of Technology, for MIKA/Doppler support. K.D. and J.D.M acknowledge funding for PV-21 programme by the EPSRC SUPERGEN Initiative.

*d.j.keeble@dundee.ac.uk

[1] B. K. Meyer, P. Omling, E. Weigel, and G. Muller-Vogt, Phys. Rev. B **46**, 15135 (1992).
[2] P. Emanuelsson, P. Omling, B. K. Meyer, M. Wienecke, and M. Schenk, Phys. Rev. B **47**, 15578 (1993).
[3] D. Verstraeten, C. Longeaud, A. Ben Mahmoud, H. J. von Bardeleben, J. C. Launay, O. Viraphong, and P. C. Lemaire, Semicond. Sci. Technol. **18**, 919 (2003).
[4] A. Carvalho, A. K. Tagantsev, S. Oberg, P. R. Briddon, and N. Setter, Phys. Rev. B **81**, 075215 (2010).
[5] T. Chanier, I. Opahle, M. Sargolzaei, R. Hayn, and M. Lannoo, Phys. Rev. Lett. **100**, 026405 (2008).
[6] S. Lany, V. Ostheimer, H. Wolf, and T. Wichert, Physica B **308–310**, 958 (2001).
[7] C. Gely-Sykes, C. Corbel, and R. Triboulet, Solid State Commun. **80**, 79 (1991).
[8] H. Kauppinen, L. Baroux, K. Saarinen, C. Corbel, and P. Hautojarvi, J. Phys. Condens. Matter **9**, 5495 (1997).
[9] R. Krause-Rehberg, H. S. Leipner, T. Abgarjan, and A. Polity, Appl. Phys. A **66**, 599 (1998).
[10] U. Reislohner, J. Grillenberger, and W. Witthuhn, J. Cryst. Growth **184**, 1160 (1998).
[11] R. Krause-Rehberg and H. S. Leipner, *Positron Annihilation in Semiconductors* (Springer-Verlag, Berlin, 1999).
[12] M. J. Puska and R. M. Nieminen, Rev. Mod. Phys. **66**, 841 (1994).
[13] F. Plazaola, A. P. Seitsonen, and M. J. Puska, J. Phys. Condens. Matter **6**, 8809 (1994).
[14] C. Corbel, L. Baroux, F. M. Kiessling, C. Gelysykes, and R. Triboulet, Mater. Sci. Eng. B **16**, 134 (1993).
[15] A. Polity, T. Abgarjan, and R. Krause-Rehberg, Mater. Sci. Forum **175–178**, 473 (1995).
[16] Z. L. Peng, P. J. Simpson, and P. Mascher, Electrochem. Solid State Lett. **3**, 150 (2000).
[17] S. Neretina, D. Grebennikov, R. A. Hughes, M. Weber, K. G. Lynn, P. J. Simpson, J. S. Preston, and P. Mascher, Phys. Status Solidi C **4**, 3659 (2007).
[18] L. Liszkay, C. Corbel, L. Baroux, P. Hautojarvi, M. Bayhan, A. W. Brinkman, and S. Tatarenko, Appl. Phys. Lett. **64**, 1380 (1994).
[19] J. D. Major, Y. Y. Proskuryakov, K. Durose, G. Zoppi, and I. Forbes, Sol. Energy Mater. Sol. Cells **94**, 1107 (2010).
[20] C. Hugenschmidt, B. Lowe, J. Mayer, C. Piochacz, P. Pikart, R. Repper, M. Stadlbauer, and K. Schreckenbach, Nucl. Instrum. Methods Phys. Res., Sect. A **593**, 616 (2008).
[21] P. Sperr, W. Egger, G. Kogel, G. Dollinger, C. Hugenschmidt, R. Repper, and C. Piochacz, Appl. Surf. Sci. **255**, 35 (2008).
[22] T. Torsti, T. Eirola, J. Enkovaara, T. Hakala, P. Havu, V. Havu, T. Höynälänmaa, J. Ignatius, M. Lyly, I. Makkonen, T. T. Rantala, J. Ruokolainen, K. Ruotsalainen, E. Räsänen, H. Saarikoski, and M. J. Puska, Phys. Status Solidi B **243**, 1016 (2006).
[23] J. Arponen and E. Pajanne, Ann. Phys. (NY) **121**, 343 (1979).
[24] E. Boroński and R. M. Nieminen, Phys. Rev. B **34**, 3820 (1986).
[25] B. Barbiellini, M. J. Puska, T. Korhonen, A. Harju, T. Torsti, and R. M. Nieminen, Phys. Rev. B **53**, 16201 (1996).
[26] B. Barbiellini, M. J. Puska, T. Torsti, and R. M. Nieminen, Phys. Rev. B **51**, 7341 (1995).
[27] See Supplemental Material at http://link.aps.org/supplemental/10.1103/PhysRevB.84.174122 for examples of the experimental positron lifetime spectra.
[28] S. Neretina, N. V. Sochinskii, P. Mascher, and E. Saucedo, Mater. Res. Soc. Symp. Proc. **864**, 567 (2005).
[29] R. A. Mackie, S. Singh, J. Laverock, S. B. Dugdale, and D. J. Keeble, Phys. Rev. B **79**, 014102 (2009).
[30] W. Brandt and R. Paulin, Phys. Rev. Lett. **21**, 193 (1968).
[31] A. Gainotti and C. Ghezzi, Phys. Rev. Lett. **24**, 349 (1970).
[32] C. Hübner, T. Staab, and R. Krause-Rehberg, Appl. Phys. A **61**, 203 (1995).
[33] T. E. M. Staab, R. Krause-Rehberg, and B. Kieback, J. Mater. Sci. **34**, 3833 (1999).